

Inelastic scattering of 40 MeV protons from ^{24}Mg . I. Natural parity transitions*

B. Zwieglinski,† G. M. Crawley, H. Nann, and J. A. Nolen, Jr.
Cyclotron Laboratory, Michigan State University, East Lansing, Michigan 48824
 (Received 15 August 1977)

Angular distributions for the inelastic scattering of protons from ^{24}Mg have been measured at a proton energy $E_p=40$ MeV with a resolution of 16 keV. The results for the natural parity states in the excitation energy range from the ground state up to $E_x\approx 13.5$ MeV are presented. The data have been analyzed using a macroscopic collective model. Coupled-channel calculations assuming the rigid-rotor model have been performed for the ground-state rotational band in ^{24}Mg . Previous conclusions on the smallness of the parameter of the hexadecapole deformation have been confirmed. The angular distribution for the 6^+ member of the ground-state rotational band at 8.120 MeV made it possible to extract the sixth order deformation parameter. Negative values of β_6 are suggested by the data. Collective model distorted-wave Born approximation calculations were performed to determine the deformation parameters β_L and isoscalar transition rates $B(IS, 0_1^+ \rightarrow L)$ for most of the observed states. Nearly half of the strength observed below $E_x=13.5$ MeV for the transitions of multipolarities $L=2, 3$, and 4 is contained in the high-energy region between $E_x=7.5$ and 13.5 MeV. Good agreement with the inelastic electron scattering data has been obtained for most of the low-energy transitions which were previously studied via (e, e') . Evidence is presented in favor of a particular spin value for a number of states for which only multiple spin assignments were previously made.

[NUCLEAR REACTIONS $^{24}\text{Mg}(p, p')$, $E=40$ MeV; measured $\sigma(E_p; \theta)$; deduced β_L 's, optical parameters. Enriched target.]

I. INTRODUCTION

In the past the nucleus ^{24}Mg has been studied by inelastic scattering quite extensively.^{1,2} These studies concentrated mainly on low-lying levels because of a lack of sufficiently good energy resolution. The present high-resolution (p, p') experiment was intended to overcome this deficiency so that angular distributions for individual levels into the region of unbound levels could be measured. Depending on how stable and similar are the shapes of the angular distributions and how well they can be fitted by distorted-wave Born approximation (DWBA) calculations, multipole transition strengths can be extracted for these higher excited states and their distribution as a function of excitation energy studied. Similar goals were pursued in a recent (α, α') experiment by Yang *et al.*³ at 70 MeV bombarding energy and in an (e, e') experiment by Johnston and Drake⁴ at 120 MeV. The energy resolution in both these experiments was in many cases not sufficient to determine the transition strength for individual levels particularly at higher excitation energies.

The nucleus ^{24}Mg is believed⁵ to have a substantial quadrupole deformation in its ground state. The determination of β_2 , the parameter for the quadrupole deformation in the ground-state rotational band of ^{24}Mg , has been the subject of numerous experiments. However the determination of the hexadecapole deformation has been attempted in only a few cases. The most recent of these are summarized in Ref. 2. The trend of the quadrupole and the hexadecapole deformations in the lower half of the s - d shell has been determined by Rebel *et al.*⁶ from the study of the inelastic scattering of 104 MeV α -particles. The hexadecapole moment is found to display a minimum at the magnesium isotopes—its value is consistent with zero. This favorable condition suggests that it might therefore be possible to determine the β_6 deforma-

tion parameter of the potential distribution about which nothing is known at present for s - d shell nuclei. This requires a high-resolution experiment in order to resolve the weakly excited $K^\pi=0^+, 6^+$ state at 8.120 MeV from the strongly excited 3^- state at 8.358 MeV. In addition, a high-resolution study of ^{24}Mg by inelastic scattering has considerable spectroscopic interest. For many states several possible spin-parity assignments have been suggested.⁷ The present experiment should help to establish unique spin assignments.

The results concerning the transitions to the natural parity $T=0$ states are the subject of the present paper. The unnatural parity states and the $T=1$ states will be discussed in a later publication. Some of the present results have been reported briefly.⁸

II. EXPERIMENTAL METHOD

The experiment was carried out using protons of energy 40.02 ± 0.02 MeV from the Michigan State University Isochronous Cyclotron. The scattered protons were detected in the focal plane of the Enge split-pole magnetic spectrometer using a 50 cm long position-sensitive proportional counter with delay-line readout.⁹ A self-supporting foil $310 \pm 20 \mu\text{g}/\text{cm}^2$ thick, enriched to 98.8% in ^{24}Mg served as a target. The data were measured relative to elastic events monitored with a NaI(Tl) detector at 90° to obtain relative angular distributions. These agreed with the cross sections obtained from the integrated charge to within 10%.

Because of the finite length of the counter and because the low lying states were generally much more intense than the states at higher excitation energy, the measurements were made in two passes. In the first series, covering the excitation energy range from the ground state up to $E_x\approx 8.5$ MeV, the angular distributions for the most intense lines in the spectrum were measured from 6°

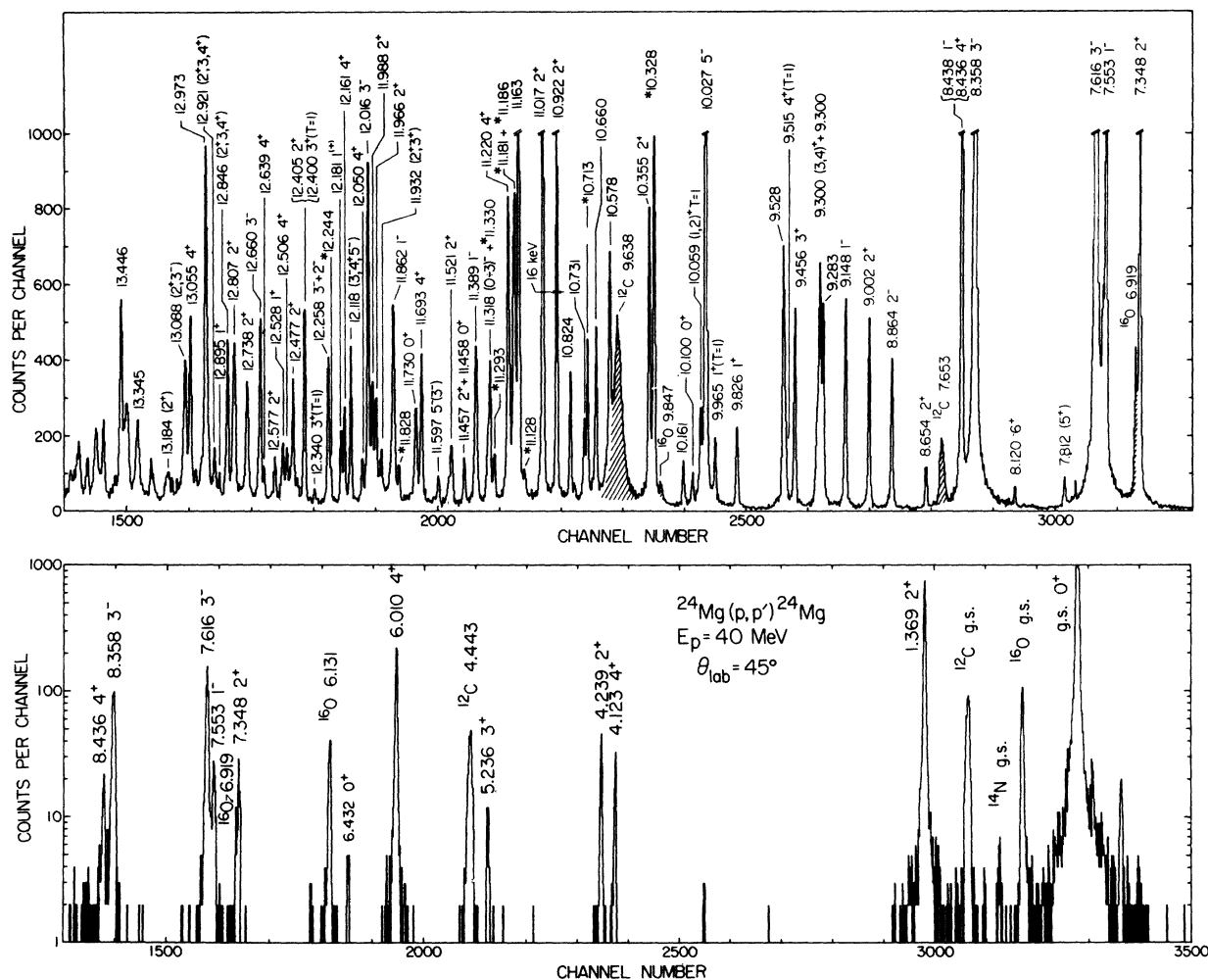


FIG. 1. Spectra of protons inelastically scattered from ^{24}Mg at the incident energy $E_p = 40 \text{ MeV}$ and the laboratory angle $\theta_{\text{lab}} = 45^\circ$. The lower spectrum was accumulated with the high-field setting of the magnetic spectrograph. Excitation energies, spins and parities labelling the peaks are generally taken from Endt and van der Leun's compilation.⁷ The modifications needed to be introduced following the results of this and other more recent work are discussed in the text. The recently^{13, 28, 29} found levels are marked by an asterisk.

to 120° in 2.5° steps. In the second series, angular distributions were measured for states with excitation energies from 4 MeV to about 13.5 MeV from 10° to 110° in 5° steps.

A sample spectrum obtained at 45° (lab) is shown in Fig. 1. The lower portion is from the first series of measurements, the upper part from the second series. The energy resolution is about 16 keV. Peak centroids and areas were extracted from the spectra via the peak fitting program FAIRFIT.¹⁰ The levels marked by an asterisk in Table II were used as calibration lines. Their energies were recently determined with a precision of $\pm 3 \text{ keV}$ by Moss.¹¹ Using these calibration lines a quadratic momentum vs position calibration curve was established via a least squares fitting procedure.¹² A list of previously known levels in ^{24}Mg from the compilation of

Endt and Van der Leun⁷ is compared with those seen in the present experiment in Table II. The precision of the determination of level positions ($\pm 7 \text{ keV}$) was limited by the differential nonlinearity of the counter. The states marked by an asterisk in Fig. 1 were found in recent experiments which are referred to in Section V. The present work represents the first attempt to determine the quantum characteristics of these new states. The statistical errors of the measurements do not exceed 3% in most cases. The cross sections have an absolute uncertainty of about 12%.

III. OPTICAL-MODEL ANALYSIS OF THE $^{24}\text{Mg}(p,p)$ ELASTIC SCATTERING

A search of the optical-model parameters was made with the automatic search program SNOOPY¹³ using the

TABLE I. Optical-model parameters for the DWBA and coupled-channel calculations.

Type	V_R (MeV)	r_R (fm)	a_R (fm)	W_V (MeV)	W_{SF} (MeV)	r_I (fm)	a_I (fm)	V_{SO} (MeV)	r_{SO} (fm)	a_{SO} (fm)
SPH ^a	38.61	1.17	0.729	12.62	0.02	1.21	0.747	6.2	1.01	0.75
DEF ^b	38.61	1.22	0.65	10.62	0.02	1.26	0.67	6.2	1.01	0.75

^aSpherical potential. Notation for the parameters as in Reference 14.

^bDeformed potential. Spherical spin-orbit part was used.

parameters of Becchetti and Greenlees¹⁴ as starting values. The elastic scattering angular distribution together with the best-fit optical-model calculation is shown in Fig. 2. The best-fit parameters labelled SPH are given in Table I. A standard notation¹⁴ is used for the parameters. Only the parameters of the imaginary part of the optical potential differ significantly from the starting values—the volume imaginary part being twice as deep as that suggested by Becchetti and Greenlees.¹⁴ This implies that the Becchetti-Greenlees potential, which was derived for nuclei with $A \geq 40$, is useful even for nuclei with $A < 40$. The potential found here is used to calculate the macroscopic collective-model inelastic DWBA cross sections as described in Sec. VI.

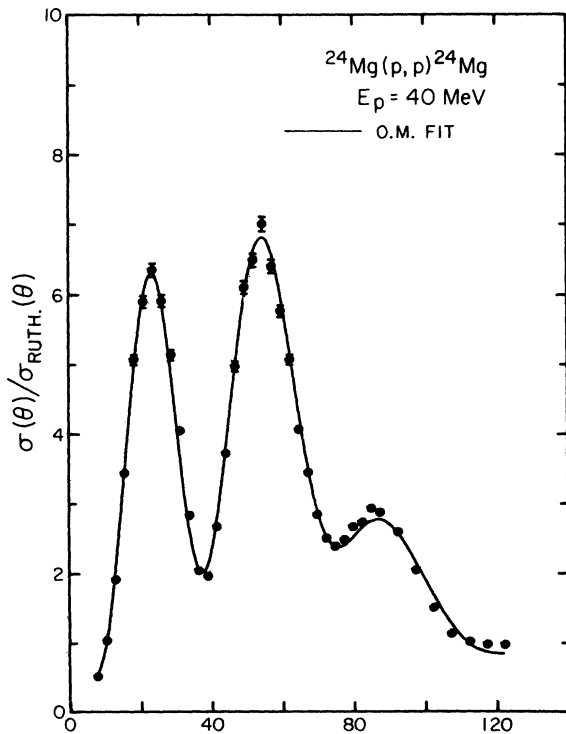


FIG. 2 Cross sections for the elastic scattering of protons from ^{24}Mg at $E_p = 40$ MeV expressed as ratios to the Rutherford cross sections. The solid line is the angular distribution calculated with the best fit optical-model parameters labelled SPH in Table I.

IV. COUPLED-CHANNEL CALCULATIONS FOR THE GROUND-STATE ROTATIONAL BAND IN ^{24}Mg

While the shape of the elastic scattering angular distribution can be fitted very well by a standard optical model calculation, the first 4^+ state at 4.123 MeV has a qualitatively different shape than other 4^+ states for example those at 6.010 MeV, 10.578 MeV and 11.693 MeV as is shown in Fig. 10. In particular, the maximum of the 4.123 MeV angular distribution is displaced by 20° to larger angles relative to other 4^+ states and the DWBA calculations. This is presumably due to the importance of the multistep excitation processes in the ground-state rotational band, and it is necessary to resort to the coupled-channel calculations to fit the angular distributions.

Coupled-channel calculations assuming a rotational-model form-factor were carried out using the program CHUCK.¹⁵ The deformation of the intrinsic potential is introduced through an explicit dependence of the radius parameters $R_{R,I} = r_{R,I} A^{1/3}$ on an angle θ relative to the nuclear symmetry axis:

$$R_{R,I}(\theta) = r_{R,I} A^{1/3} \left(1 + \sum_{\lambda=2}^{\lambda_{\max}} \beta_{\lambda} Y_{\lambda 0}(\theta) \right), \quad (1)$$

where β_{λ} are the deformation parameters. Deformations up to the sixth order are taken into account in the present calculations. The diffuseness of the intrinsic potential is expected to be smaller than for the phase-equivalent spherical case and the imaginary depth should be smaller since some of the flux lost from the entrance channel is explicitly taken into account by the coupled-channel method. With the radii readjusted to give a subjectively best-fit to the elastic scattering data the potential labelled DEF in Table I was obtained. The elastic angular distribution calculated with this potential is compared with the data in Fig. 3a. The spin-orbit part was not deformed, it was assumed to be identical to the spin-orbit part in the potential labelled SPH in Table I. The parameters obtained for the central part of the potential depend on whether or not the spin-orbit part is used in fitting the potential to the elastic data. Thus the spin orbit potential effects the deformation parameters in an indirect way.

Two series of calculations were performed for the ground state rotational band. In the first calculations, the spin-orbit potential was included and only the couplings indicated in the inset of Fig. 3(b) were taken into account. In particular the only $L=4$ and $L=6$ couplings included were those connecting the ground state with the 4^+ and 6^+ members of the ground-state band. The β_2 parameter was determined by normalizing the calculated cross section for the 2^+ 1.369 MeV state to the experimental cross section at 25° . The positive sign of β_2 was assumed following the recent measurement¹⁶ of the quadrupole moment for the 2^+ state. In contrast to the

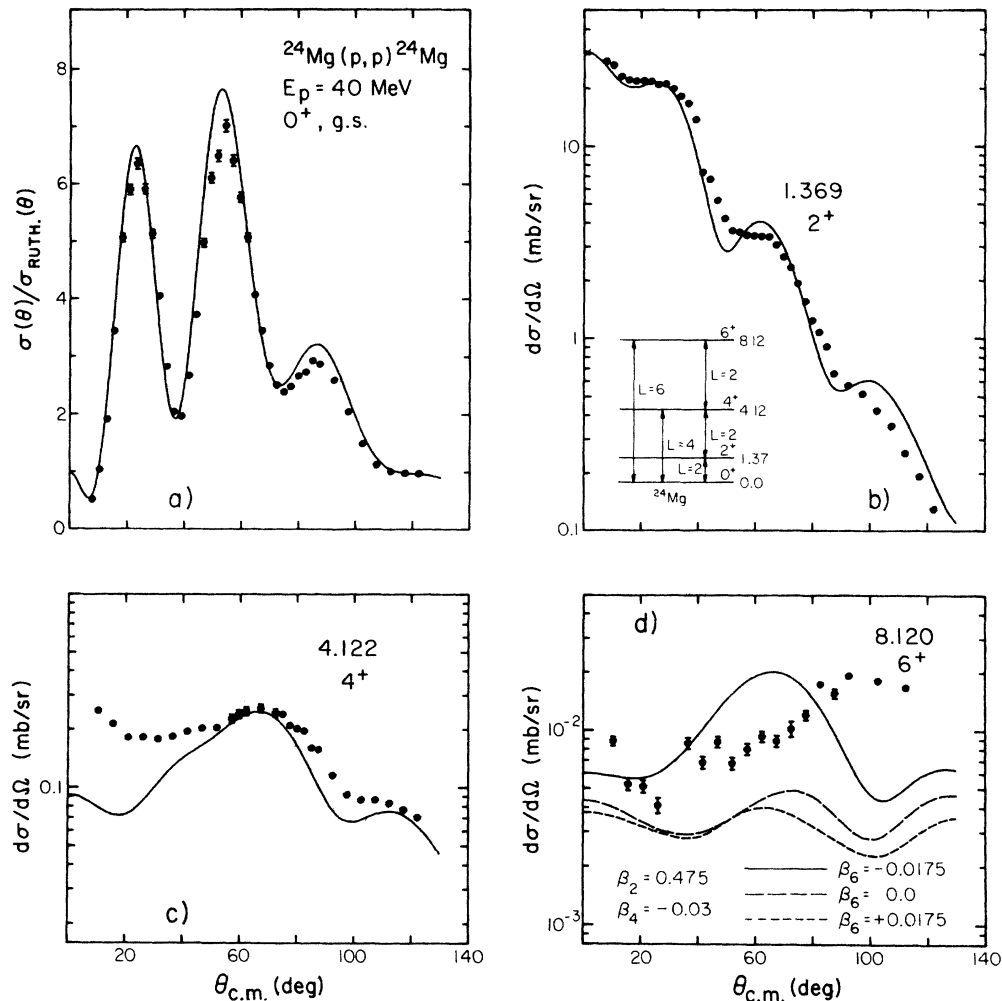


FIG. 3 (a-d) Inelastic scattering angular distributions for the states of the ground-state rotational band in ^{24}Mg compared with the predictions of the coupled-channel calculations with the spin-orbit terms in the potentials included. The coupling terms included in these calculations are shown schematically in the inset to Fig. 3b. The deformation parameters used in the calculations are indicated in Fig. 3d. Only for the 6^+ state are the theoretical angular distributions, corresponding to the three indicated β_6 values, significantly different.

higher band members, the cross sections for the 2^+ state depend in a fairly linear way on β_2 . The value of $\beta_4 = -0.03$ was chosen to match the calculated cross section for the 4^+ , 4.122 MeV state with the experimental maximum at around 70° . The angular distribution of the 6^+ state at 8.120 MeV is compared in Fig. 3d with the angular distributions calculated for three different values of β_6 . The calculations for $\beta_6 = 0$ (long dashes) clearly demonstrate that quadrupole and hexadecapole deformation alone are not sufficient to reproduce the data. With a positive β_6 (short dashes) the one-step $L=6$ excitation component destructively interferes with the three-step $L=2$, leading to cross section values even lower than those obtained with $\beta_6 = 0$ in the angular range around 90° in which the experimental maximum is located. For a value of $\beta_6 = -0.0175$, the magnitude of the maximum in the experimental cross section is reproduced by the theoretical calculation (solid line in Fig. 3d) but the location of the maximum is predicted to be at a c.m. angle of 66° instead of around 90° as observed experimentally.

Testing the influence of the hexadecapole deformation

on the angular distribution for the 6^+ state was the main purpose of the second series of calculations. The spin-orbit potential was therefore neglected, and the maximum number of $L=4$ couplings was taken into account (see the inset to Fig. 4e). The results for the 4^+ and 6^+ states are presented in Figs. 4a-f. Neither a small positive (Figs. 4a-b) nor small negative (Figs. 4e-f) value of β_4 is uniquely indicated by a comparison of the prediction with the 4^+ angular distribution. The negative sign for β_4 gives a better description of the 4^+ angular distribution at backward angles, whereas the agreement is better at forward angles with a positive sign of β_4 . Note also that neglecting the spin-orbit potential has a comparatively minor effect on the predicted cross sections as can be seen by comparing the calculations in Fig. 3c and 3d with spin-orbit included to those in Fig. 4a and 4b which exclude the spin-orbit potential. Irrespective of the choice of the sign of the β_4 parameter, the calculations yield a minimum around 90° in the angular distribution for the 8.120 MeV 6^+ state when a positive β_6 is assumed. Only with $\beta_6 < 0$ can a maximum in cross section be

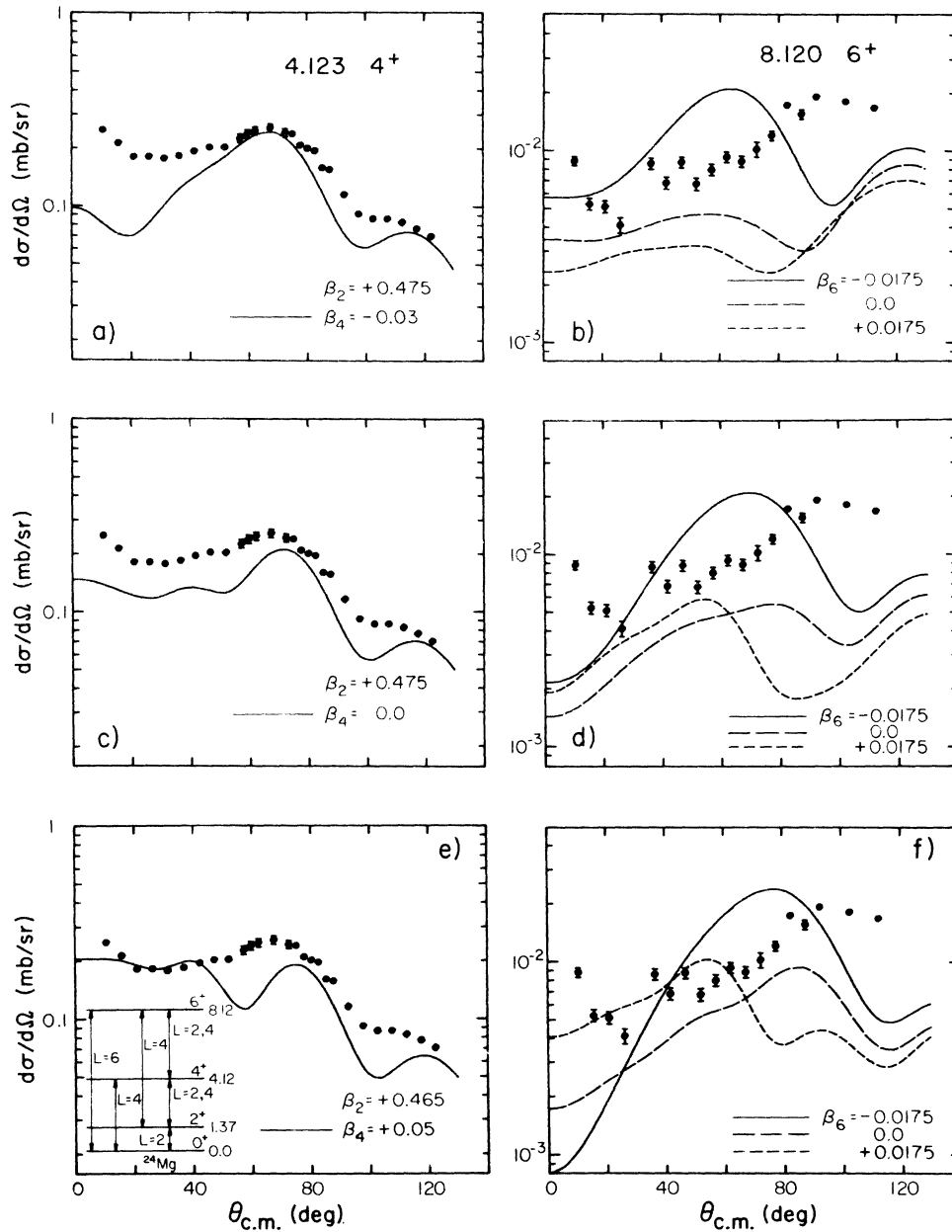


FIG. 4 (a-d) Comparison of the angular distributions for the inelastic scattering of protons to the 4.122 MeV 4^+ and 8.120 MeV 6^+ ground-state band members with the results of the coupled-channel calculations. The couplings indicated in the inset to Fig. 4e have been taken into account. Spin-orbit term in the distorting potentials has not been included. Figs. 4a-b correspond to $\beta_2 = 0.475$, $\beta_4 = -0.03$, Figs. 4c-d correspond to $\beta_2 = 0.475$, $\beta_4 = 0$ and Figs. 4e-f correspond to $\beta_2 = 0.465$, $\beta_4 = 0.03$. For the 8.120 MeV 6^+ state the calculated curves corresponding to each of the three indicated β_6 values are plotted.

obtained at backward angles as implied by the experimental angular distribution. The conclusion is that the angular distribution for the 6^+ state is mostly determined by the three-step $L=2$ and the one-step $L=6$ excitations and independent of β_4 when the latter is changed within the limits imposed by the cross sections for the 4^+ state. The rigid-rotor model assumed in the present coupled-channel calculations does not give detailed agreement with the data, and thus the value obtained ($\beta_6 = -0.0175$)

should be treated at tentative. The discrepancies may indicate that the $K^\pi = 0^+$ band cannot be treated as isolated and that the mixing with e.g. the $K^\pi = 2^+$ band should be explicitly taken into account. However a better fit to the 4^+ state was found for 104 MeV (α, α') scattering when the calculations include only the $K^\pi = 0^+$ band. This may indicate that since 40 MeV protons have a much longer mean free path in nuclear matter, a better knowledge of the transition densities in the important

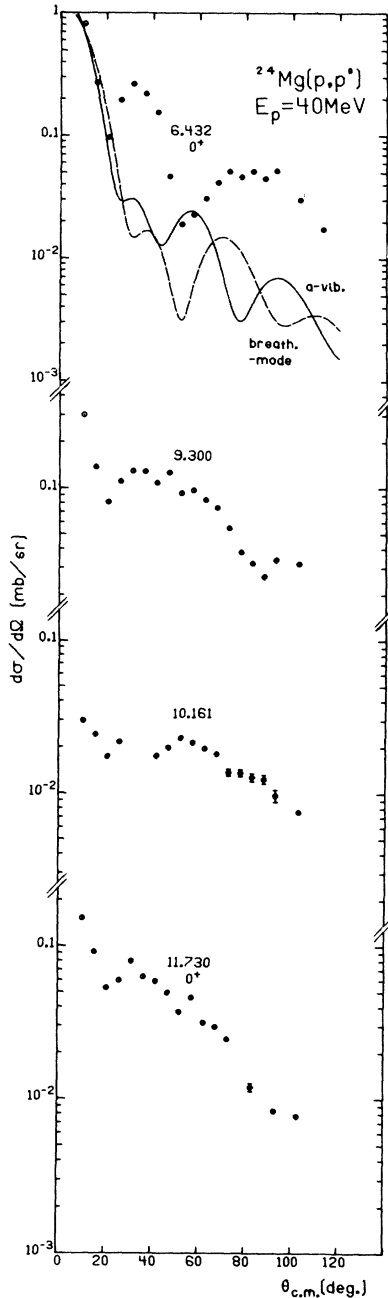


FIG. 5 Angular distributions for the states of the known and suggested characteristics $J^\pi=0^+$. The solid line compared with the 6.432 MeV angular distribution was calculated with the "a-vibration" macroscopic form factor (7). The dashed line corresponds to the "breathing-mode" form factor.

surface region of the nucleus is required. Coupled-channel calculations with transition densities calculated from shell-model wave functions would be a way of testing this assumption.

V. DISCUSSION OF SPIN-PARITY ASSIGNMENTS

For a number of the observed states no spin-parity assignments exist at present. They are classified into

groups with other states with known quantum characteristics primarily on the basis of the similarity of shapes of the angular distributions. Since the strong coupling effects are probably not limited to the ground-state rotational band (see Sec. VII) the assignments made on this basis are only tentative and require further confirmation by standard spectroscopic methods. The levels of special interest with regard to spin and parity assignments are discussed briefly below. The levels studied in the present work in the energy range from 10.682 to 13.446 MeV were previously investigated with the α -particle induced resonance reactions.¹⁷⁻²⁰ These excite selectively the natural parity states with isospin $T=0$. Most of the states in this energy range for which the transition rates are determined in Sec. VII have their counterparts among the α -induced resonances. Those few cases which do not have counterparts and thus may suggest either unnatural parity and/or isospin $T=1$ are also discussed in this section.

$$E_x=8.436 \text{ MeV } 4^+ \text{ and } E_x=8.437 \text{ MeV } 1^- \text{ levels}$$

The angular distribution corresponding to this unresolved doublet (see Fig. 6) is nearly identical to the well established 1^- state at 11.390 MeV. This suggests that the lower spin member gives the main contribution to the sum.

$$E_x=9.148 \text{ MeV } 1^- \text{ level}$$

The angular distribution for this state has a characteristic bell shape unlike to the rest of the 1^- states in Fig. 6 but similar to other negative parity states which share the common feature that they are strongly excited in the proton transfer $^{23}\text{Na}(d,n)^{24}\text{Mg}$ reaction.^{21,22} The state in question has a large $l_p=3$ component. This suggests that states of this type are particle-hole excitations formed by nucleon promotion from the $(1d,2s)$ to the $(1f,2p)$ shell. The $1p$ -shell hole components (e.g. of the type $(1d_{5/2}, 1p_{3/2}^{-1})$) of these negative parity states can be also excited via the $^{24}\text{Mg}(p,p')^{24}\text{Mg}$ reaction. These are not accessible for study in the $^{23}\text{Na}(d,n)^{24}\text{Mg}$ reaction. The differences in the shapes of the angular distributions (for the same angular momentum transfer) seen in (p,p') reaction reflect the differences in transition densities between these single-particle and collective excitations. A discussion of these excitations in the framework of the microscopic approach will be given in a later publication.^{2,3}

$$E_x=9.282 \text{ MeV } 2^+ \text{ level, } E_x=9.300 (3,4)^+ \\ \text{and } E_x=9.300 (4^-) \text{ levels}$$

Peaks corresponding to a state at 9.282 MeV and a state or states at 9.300 MeV are clearly resolved in the present experiment (see Fig. 1). The angular distribution for the 9.282 MeV peak is presented in Fig. 11 to stress the similarity of its angular distribution with the known^{24,25} 5^- state at 10.027 MeV rather than with the 2^+ states (Figs. 7 and 8). A 9.280 MeV group excited by both $l_p=1$ and $l_p=3$ transfers has been observed by Tang, et al.²² in the $^{23}\text{Na}(d,n)^{24}\text{Mg}$ reaction. Thus the particle-hole character of one of the triplet members is highly probable. In none of the previous spin-parity assignments^{24,26} have the states belonging to the 9.30 MeV triplet been resolved. A spin parity of 4^- is suggested as the most probable assignment for the negative parity member of the triplet.²⁴ The evidence from the present work is that the negative parity particle-hole excitation corresponds to the 9.282 MeV member of the triplet. The predictions of the microscopic^{2,3} calculations assuming a $(1f_{7/2}, 1d_{5/2}^{-1})$ configuration and $J^\pi=4^-$ for the 9.282 MeV state are in reasonable agreement with the

angular distribution presented in Fig. 11. The group corresponding to the 9.300 MeV doublet has a cross section which rises rapidly towards zero degrees resembling in this respect other 0^+ states in ^{24}Mg (see Fig. 5). Johnston and Drake⁴ have measured the inelastic (e,e') form factor for the 9.29 MeV complex and concluded that it contains a state with spin-parity of either 0^+ or 2^+ . The present data corroborate the 0^+ assignment for one of the states of the 9.300 MeV doublet. However the lack of a very consistent shape for the 0^+ angular distributions except for the strong rise at very forward angles makes it

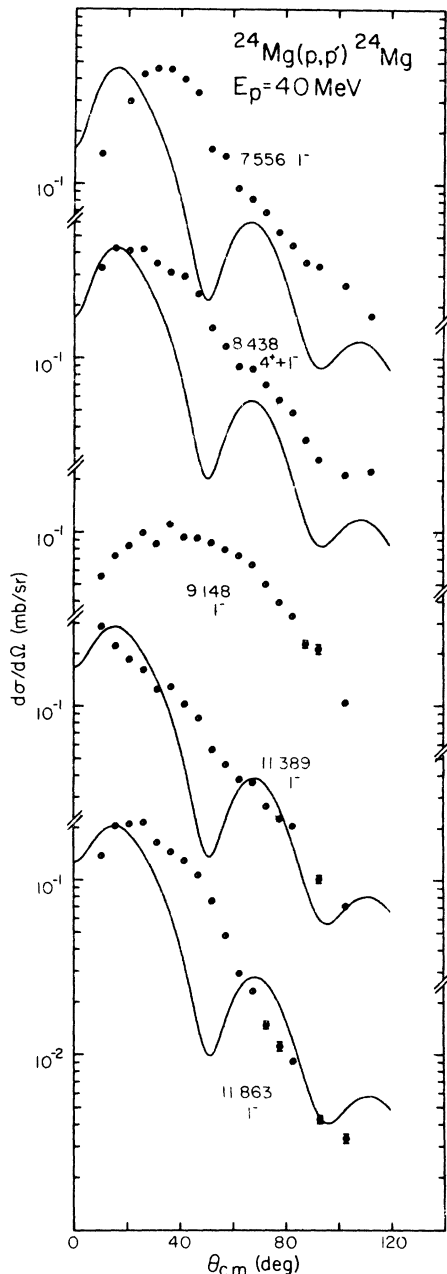


FIG. 6 Angular distributions for the states with $J^\pi=1^-$. Solid lines are the DWBA cross sections calculated with the form factor (7).

difficult to estimate the amount of strength which could be present from an unresolved 3^+ or 4^+ state.

$$E_x=9.515 \text{ MeV } 4^+ \text{ T=1 level and } E_x=9.520 \text{ MeV } (6^+) \text{ level}$$

The peak-fitting program decomposes this peak in the spectrum (Fig. 1) into two components. The 9.520 MeV component has an angular distribution similar to the 2^+ states. This is shown in Fig. 7 together with the L=2 DWBA prediction. Moss¹¹ reports a triplet of states with energies 9.514, 9.521 and 9.528 MeV. The suggested 2^+ state corresponds probably to the most strongly excited 9.528 MeV state seen by Moss. The 9.521 MeV (6^+) component is weakly excited in his (p,p') spectrum at a bombarding energy of 20 MeV and seems to be weakly excited also in the present experiment.

$$E_x=10.027 \text{ MeV } 5^-(3^-) \text{ level}$$

Branford et al.²⁴ consider that $J^\pi=5^-$ characteristics is the most probable spin assignment. The present data (see Fig. 11) also favour a 5^- character for this level rather than 3^- which would give an angular distribution with a maximum around 35° (see Fig. 9 for the transitions with an L=3 transfer).

$$E_x=10.328 \text{ MeV and } E_x=10.355 \text{ MeV } 2^+(0^+) \text{ levels}$$

The existence of a doublet around these energies was suggested by Johnston and Drake⁴ who concluded that the form factor for the 10.35 MeV complex is not compatible with a single L=2 multipolarity. A second state with either $J=3^-$ or 4^+ was required in addition to the previously studied 10.355 MeV state. The present data rule out the 4^+ assignment since 4^+ states have angular distributions which peak around 45° (see Fig. 10). Both L=3 and L=2 are compatible with the present measurements for the 10.328 MeV state (see Fig. 7). The 10.355 MeV angular distribution definitely favors a 2^+ assignment since the sharp rise in the cross section towards zero degrees which is observed for all of the observed 0^+ states (Fig. 5) is lacking in this case.

$$E_x=10.578 \text{ MeV level}$$

The angular distribution for this state is compatible with an L=4 transfer and therefore we suggest $J^\pi=4^+$ (see Fig. 10).

$$E_x=10.660 \text{ MeV and } E_x=10.680 \text{ MeV } 0^+ \text{ levels}$$

The 10.680 MeV 0^+ state was excited with measurable cross sections only at extreme forward angles (at 10° and 19°) in the present experiment. The angular distribution for the 10.660 MeV state is consistent with an angular momentum transfer of L=4 (see Fig. 10). The only other information²⁷ on this state is that it decays by γ -emission mainly to the 2^+ state at 1.369 MeV. This does not contradict the $J^\pi=4^+$ assignment but still leaves the possibility of $J^\pi=3^+$.

$$E_x=10.713 \text{ MeV level and } E_x=10.731 \text{ MeV level}$$

It has been recently demonstrated^{28, 29} that the analog of the 1.346 MeV 1^+ level in ^{24}Na should be associated with the 10.713 MeV member of this doublet rather than with the 10.731 MeV state as has been previously⁷ assumed.

$$E_x=10.824 \text{ MeV level}$$

A DWBA angular distribution with L=4 gives a satisfactory fit to the experimental data for this state (see Fig. 10). This state was not excited in the $^{20}\text{Ne}(\alpha,\gamma)$ reaction. It could be a candidate for an isobaric analog of

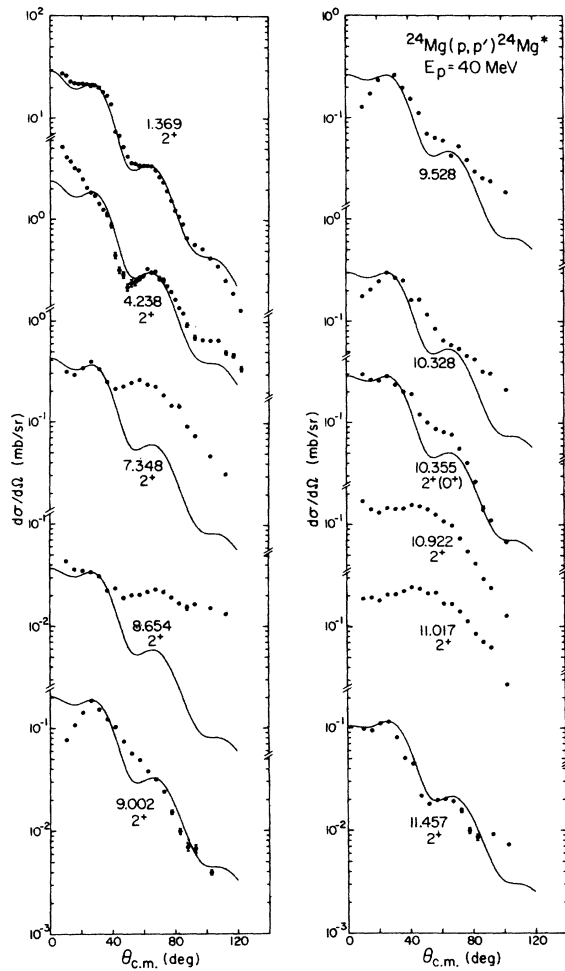


FIG. 7 Angular distributions for the states in the excitation energy range from $E_x = 1.369$ MeV to $E_x = 11.457$ MeV compared with the DWBA calculations for angular momentum transfer $L=2$ (solid lines). The deformation parameters extracted from normalizing theory to the data are collected in Table II.

the 3^+ 1.344 MeV (Ref. 30) state in ^{24}Na . It is located only 26 keV below the expected position of the analog at 10.860 MeV. A much larger shift (150 keV) is observed for the analogs of the 1^+ and 2^+ members of the 1.34 MeV triplet in ^{24}Na due probably to a significant s-wave parentage of these two states. The 3^+ $T=1$ state can be excited with $L=4$ if both spin and isospin are flipped in the (p,p') reaction.

$E_x = 11.168$ MeV $(1-3)^-$ level, $E_x = 11.181$ MeV
and 11.186 MeV levels

Large peaks are observed at 11.163 and 11.181 MeV (Fig. 1) as well as the peak corresponding to the known 4^+ state at 11.220 MeV. The peak observed at 11.163 MeV has an $L=3$ characteristic shape (see Fig. 9). $L=3$ strength around 11.0 MeV was required also in the (e,e') experiment.⁴ The peak at 11.181 MeV represents one or both members of the 11.181, 11.186 MeV doublet recently discovered by Moss.¹¹ A DWBA angular distribution with $L=3$ offers a satisfactory fit (Fig. 9) to the angular

distribution of this probably complex peak. None of these two states was previously detected with the $^{20}\text{Ne}(\alpha,\gamma)^{24}\text{Mg}$ reaction.¹⁸ One of the 11.181, 11.186 MeV doublet members may correspond to the 11.188 MeV state which was found in the $^{23}\text{Na}(d,n\gamma)^{24}\text{Mg}$ work by Porterfield and Ritter.³¹ They suggested that this state had isospin $T=1$.

$E_x = 11.293$ MeV level

This state was not excited in the $^{20}\text{Ne}(\alpha,\gamma)^{24}\text{Mg}$ reaction.¹⁸ The maximum of the angular distribution occurring around the c.m. angle of 80° (see Fig. 11) implies that a high angular momentum transfer is involved in the excitation of this state. For the sake of comparison, an $L=6$ DWBA angular distribution is superimposed on the data in Fig. 11. The bell-shaped angular distribution may suggest that a particle-hole excitation is observed. The state in question could be a candidate for the $J^\pi=6^-$ member of the $(1f_{7/2}1d_{5/2}^{-1})$ $T=0$ multiplet. In fact the $J^\pi=6^-$ $T=0$ states occur around this energy in both $^{20}\text{Ne}(E_x=10.609$ MeV)⁷ and $^{28}\text{Si}(E_x=11.577$ MeV)³² nuclei. The existence of a strong analog-antianalog $M1$ γ -transition to this state from the now well established 6^+ , 2^+ , 3^+ , 3^+ $J^\pi=6^-$ $T=1$ state at 15.1-MeV would confirm this hypothesis.

$E_x = 11.318$ MeV $(0-3)^-$ level and 11.330 MeV level

A doublet of closely spaced levels is excited around this energy as was first demonstrated by Moss.¹¹ We were able to extract the angular distribution only for the dominating 11.318 MeV component of the peak. This angular distribution is consistent with an $L=3$ transfer (see Fig. 9). We suggest $J^\pi=3^-$ for the 11.313 MeV state.

$E_x = 12.400$ MeV 3^+ and $E_x = 12.405$ MeV 2^+ level

There is apparently a significant contribution of the 3^+ state to the cross section for this unresolved doublet, since the maximum of the angular distribution is displaced from 30° towards larger angles. Meyer *et al.*²⁷ ascribe $T=1$ to the 12.400 MeV state.

$E_x = 12.846$ MeV $(2^+, 3, 4^+)$ level

Neither an $L=3$ nor $L=4$ DWBA angular distribution (see Fig. 8) fits the data particularly well. The experimental angular distribution is very similar to the angular distribution for the known 12.660 MeV $J^\pi=3^-$ state. Thus $J^\pi=3^-$ is preferred.

$E_x = 12.973$ MeV level

The peak corresponding to the $E_x = 12.973$ MeV level dominates this part of the spectrum (see Fig. 1). The angular distribution is consistent with an $L=4$ pattern (see Fig. 10). The same state has probably been seen by Spear and Wright¹⁹ as a strong resonance in the $^{20}\text{Ne}(\alpha,\alpha')^{20}\text{Ne}^*$ (1.63 MeV) reaction and in the $^{20}\text{Ne}(\alpha,p)^{23}\text{Na}$ (0.44 MeV) reaction thus implying that its isospin is $T=0$. They concluded that the quantum numbers $J^\pi=4^+$ or 5^- are most likely for this state. Stark *et al.*³⁵ have assigned $J^\pi=2^-$ using different techniques. The present data tend to support the $J^\pi=4^+$ assignment.

$E_x = 13.050$ MeV $4^+, (2^+)$ level

The angular distribution is compared in Fig. 10 with the $L=4$ DWBA predictions. The shape of the angular distribution is closer to $L=4$ than to $L=2$, thus $J^\pi=4^+$ is preferred.

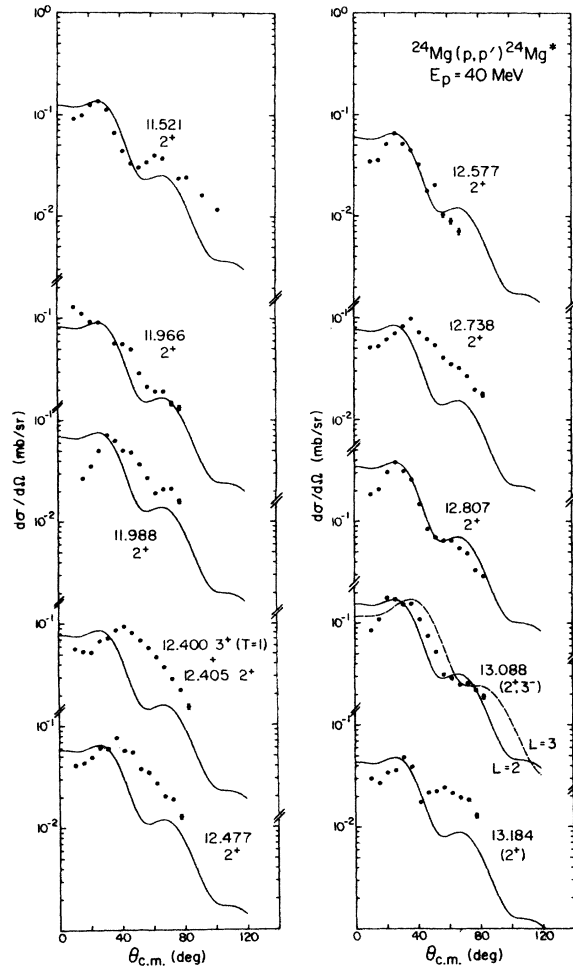


FIG. 8 Angular distributions for the states in the excitation energy range from $E_x=11.521$ to 13.184 MeV compared with the DWBA calculations for angular momentum transfer $L=2$ (solid lines). For the 13.088 MeV state both the $L=2$ and $L=3$ (dashed line) cross sections are presented. The deformation parameters extracted from normalizing theory to the data are collected in Table II.

$E_x=13.088$ MeV ($2^+, 3^-$) level

The data are not conclusive as to which is the preferred spin value (see Fig. 8). Both $L=2$ and $L=3$ transfers are shown for comparison.

$E_x=13.446$ MeV ($1, 2$) level

The angular distribution shown in Fig. 9 is quite well fitted by an $L=3$ angular distribution. This disagrees with the previous assignment of $J^\pi=(1,2)$ made by Meyer et al.²⁷ The state has also been seen in the reactions $^{12}\text{C}(^{16}\text{O},\alpha)$ (Ref. 25) and $^{20}\text{Ne}(\alpha,\gamma)$ (Ref. 20). However, no spin-parity assignments were made.

VI. ISOSCALAR TRANSITION RATES IN ^{24}Mg FROM

$^{24}\text{Mg}(p,p')^{24}\text{Mg}^*$ AND THE DWBA ANALYSIS

While the coupled channel effects are clearly important within the ground state band, as was shown in Sec. IV it is

of interest to see how well a one step DWBA calculation will work for the natural parity $T=0$ states in ^{24}Mg . Therefore the angular distributions for the $^{24}\text{Mg}(p,p')^{24}\text{Mg}$ reaction to the natural parity $T=0$ states in ^{24}Mg have been compared with the predictions of the DWBA theory. The DWBA cross sections for the angular momentum transfer $L, \sigma_L(\theta)$, are calculated with the macroscopic collective model form factors using the code DWUCK.³⁶ Coulomb excitation was included. The potential parameters labelled SPH in Table I were used in the calculations and complex coupling has been assumed. The experimental data are compared with the DWBA predictions in Figs. 5 to 11. Normalizing the theoretical cross section to the experimental angular distribution $\sigma_{\text{ex}}(\theta)$ yields the deformation parameter β_L from the equation:

$$\sigma_{\text{ex}}(\theta) = \beta_L^2 \sigma_L^{\text{DW}}(\theta). \quad (2)$$

The values of β_L extracted are given in Table II.

In order to determine the isoscalar transition strength, the mass deformation parameter $\beta_L(m)$ is required. This parameter is related to the potential deformation parameter β_L by the equation^{37,38}

$$\beta_L R = \beta_L(m) R_m, \quad (3)$$

where R is the larger of the real and imaginary potential radii and R_m is the radius of mass distribution taken as $1.20A^{1/3}$ fm. The ratio of the isoscalar transition rate, $B(\text{IS}, 0^+ \rightarrow L)$ to the single particle transition rate $B_{\text{s.p.}}(L)$ is given by:³⁸

$$G_L = \frac{B(\text{IS}, L)}{B_{\text{s.p.}}(L)} = \beta_L(m)^2 \frac{(L+3)^2 Z^2}{4\pi(L+1)} K_L \quad (4)$$

where K_L is a constant which gives the correct transition rate for the more realistic Fermi distribution instead of a uniform mass distribution for a given multipolarity L . The values of K_L are tabulated by Bernstein.³⁸ The values of G_L determined in the present work are listed in Table II and are compared with the isoscalar transition rates obtained from (α, α') measurements and with electromagnetic transition rates from (e, e') .

Another quantity of interest is the fraction of the energy-weighted sum rule (EWSR) limit for a particular multipole contained in the observed transitions. The sum of the energy weighted transition strengths is given by:

$$S_L = \sum_f G_L^f E_f \quad (5)$$

where the sum is taken over all final states f of energy E_f reached by a particular multipolarity L . The values of S_L , the EWSR limit, again corrected for a Fermi mass distribution, are taken from Bernstein's³⁸ tabulation. The fraction of the EWSR exhausted is then given by the ratio S_L/S_L and is discussed in Section VII.

VII. DISCUSSION OF MULTIPOLE TRANSITIONS

Transitions with $L=0$

Angular distributions for the states known to have $J^\pi=0^+$ and the states for which the angular distributions are suggestive of $J^\pi=0^+$ are shown in Fig. 5. The characteristic feature of these angular distributions is their rapid rise at small angles. Satchler^{39,40} has proposed a generalization of the standard macroscopic collective model to allow the calculation of monopole vibrations. In his approach all three parameters describing the nuclear potential, V , R and a are allowed to vibrate as opposed to the traditional model in which only R -vibrations are considered. The requirement that the

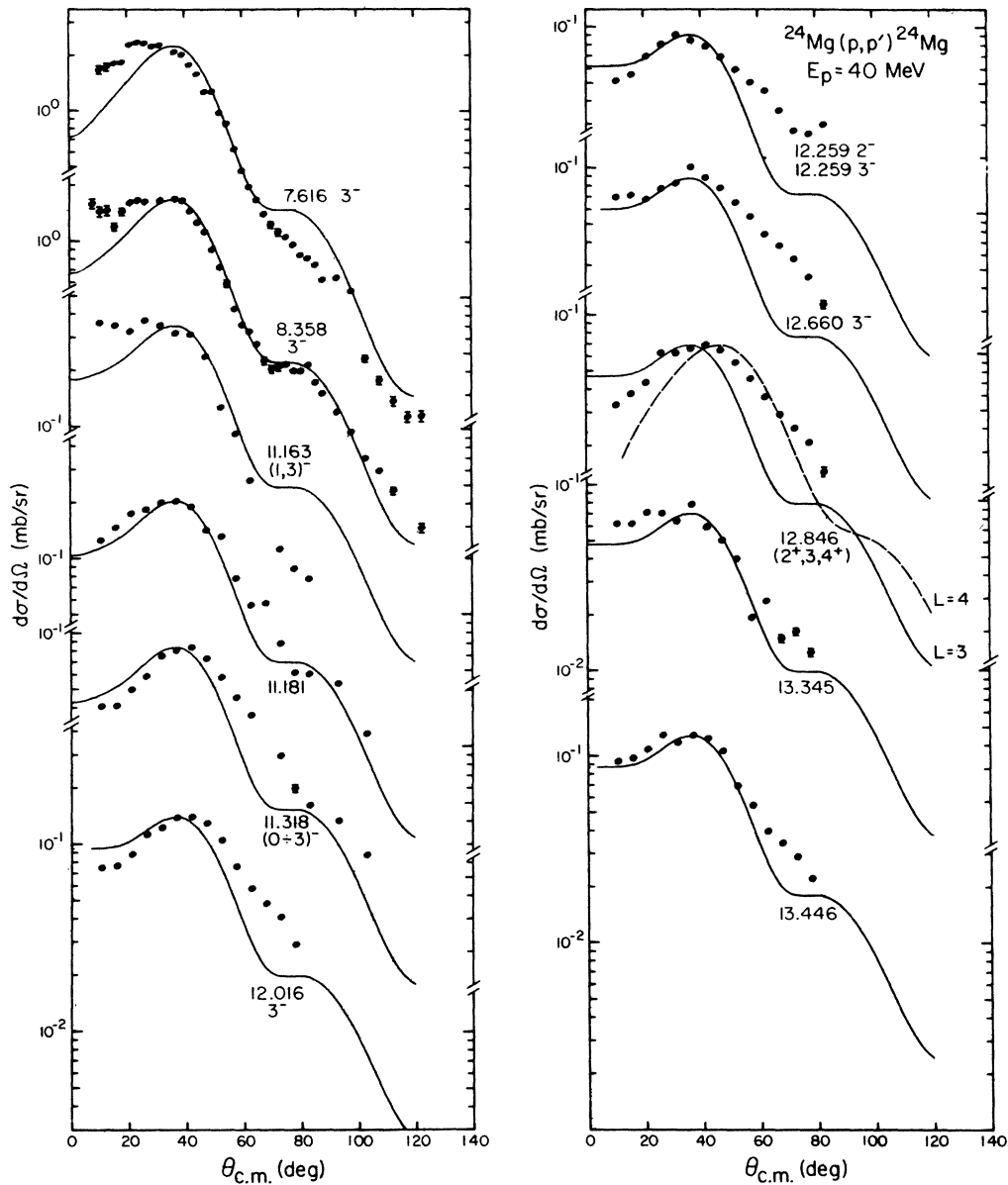


FIG. 9 Angular distributions compared with the DWBA calculations for angular momentum transfer $L=3$ (solid lines). For the 12.846 MeV state the cross sections corresponding to both the $L=3$ (solid line) and $L=4$ transfers (dashed line) are presented. The normalization coefficients β_L are tabulated in Table II.

volume integral of the potential should be preserved in the vibration yields a relation between the increments δV , δR and δa :

$$\delta R \int (\partial U / \partial R) r^2 dr + \delta V \int (\partial U / \partial V) r^2 dr + \delta a \int (\partial U / \partial a) r^2 dr = 0. \quad (6)$$

In the particular form ("a-vibration") of the transition potential, $\Delta U(r)$, used in the present work only the increments δR and δa were considered:

$$\Delta U(r) = \frac{V}{a} \left[\delta R + \frac{r-R}{a} \delta a \right] \frac{df}{dx} \quad (7)$$

where $f(x)$ is the Woods-Saxon form factor. The DWBA angular distribution for the 6.432 MeV state calculated with the form factor (7) is shown in Fig. 5 (solid line). The integrals entering (6) were calculated numerically. The

deficiency of the DWBA angular distribution is the too frequent oscillation. A somewhat better description is offered by the "breathing mode"⁴⁰ form factor (dashed line). However, the oscillatory structure of the data is still not reproduced.

In view of the discrepancies we have not attempted to extract quantitative information from other transitions with $L=0$. A better description is expected⁴¹ on the basis of the microscopic model.

Transitions with $L=1$

The dipole transitions with $T=0$ also require a nonstandard approach since the $L=1$ term of the R-vibration corresponds to a spurious translation of the center of mass

TABLE II. (Continued)

E ^a (MeV)	J ^π ^a	E _x ^b (MeV)	L ^b	β _L ^b	B(0 ₁ ⁺ →L)/B _{S.P.} (L)				
					(p,p') ^b 40 MeV	(α,α') ^c 70 MeV	(e,e') ^d	(e,e') ^e	(e,e') ^f
11.521	2 ⁺	11.520	2	0.052	0.16				
11.597	5 ⁻ (3 ⁻)	11.596							
11.693	4 ⁺	11.694 [*]	4	0.055	0.47				
11.730	0 ⁺	11.727	0						
11.863	1 ⁻	11.860	1	0.059				1.42	
11.966	2 ⁺	11.965	2	0.043	0.10	0.41			
11.988	2 ⁺	11.990	2	0.039	0.086				
12.016	3 ⁻	12.016 [*]	3	0.067	0.39			0.50	
12.050	4 ⁺	12.050	4	0.030	0.14				
12.118	(3 ⁻ ,4 ⁺ ,5 ⁻)	12.124							
12.167	4 ⁺	12.157	4	0.046	0.33				
12.259	2 ⁻ +3 ⁻	12.261	3	0.054	0.26				
12.400	3 ⁺ (T=1)								
12.405	2 ⁺	12.402 [*]	2	0.041	0.098				
12.420	7 ⁻								
12.462	1 ⁻								
12.477	2 ⁺	12.470	2	0.036	0.074				
12.506	4 ⁺	12.508	4	0.030	0.14				
12.577	2 ⁺	12.578	2	0.036	0.075	0.43		0.107	
12.638	4 ⁺	12.641	4	0.030	0.15				
12.660	3 ⁻	12.663	3	0.053	0.25				
12.738	2 ⁺	12.739	2	0.041	0.097				
12.774	0 ⁺								
12.807	2 ⁺	12.812	2	0.087	0.44	0.61			
12.846	(2 ⁺ ,3,4 ⁺)	12.850	3	0.047	0.19				
			4	0.056	0.50				
12.973	4 ⁺ ,5 ⁻	12.973 [*]	4	0.094	1.39				
13.050	4 ⁺ ,(2 ⁺)	13.059	4	0.062	0.61				
13.088	(2 ⁺ ,3 ⁻)	13.088	2	0.058	0.20			0.18	
			3	0.074	0.48				
13.184		13.181	2	0.031	0.055				
13.344	3 ⁻	13.344	3	0.047	0.20				
13.446		13.440	3	0.064	0.36				

^aReference 7.^bPresent work.^cReference 3.^dReference 44.^eReference 4.^fReference 45.^gThese values are from the coupled channel calculation.

of the entire nucleus.³⁹ The transition potential (7) was used to calculate the $L=1$ angular distributions. The condition relating the oscillation of the diffuseness δa to the oscillation of the radius δR corresponds in the case of $L=1$ to the requirement that the center of mass of the system remains fixed during the excitation.³⁹ The experimental angular distributions are compared in Fig. 6 with the DWBA calculations. The transition potential (7) offers a slightly better description for the $L=1$ transitions than the transition with $L=0$ as one can see from the comparison. However, the experimental angular distributions decrease monotonically with angle while the theoretical cross sections have strong oscillations superimposed on the general decrease with angle.

An alternative interpretation for the 1^- $T=0$ states is that they represent compressional modes of the nucleus.^{4,2,43} The difficulty associated with such an interpretation is that a much lower estimate for the velocity of sound in nuclear matter is obtained⁴³ than suggested by other data. An interesting consequence⁴² of the fixed center of mass condition for the inelastic electron scattering is the "E3-like" dependence of the form factor-squared on the momentum transfer. It is argued further in this section that this may lead to some confusion in the extraction of the ratios of excitation strengths for the 3^- 8.358 MeV and 7.616 MeV states in (e,e') experiments since the 3^- states are not resolved from their 1^- neighbors.

Transitions with $L=2$

The numerical values of the transition rates are compared in Table II with values from (α,α') and (e,e') experiments.^{4,44,45} The distribution of the quadrupole transition strength versus excitation energy in ^{24}Mg is shown in Fig. 12. The fraction of the energy-weighted sum-rule exhausted up to an excitation energy about 13.5 MeV is shown in Fig. 13. About 30% of the EWSR limit is contained in the observed transitions. Nearly half of this is contained in the lowest two 2^+ states at 1.369 and 4.239 MeV. The remaining part is distributed rather uniformly over the energy range from 7.35 to 13.5 MeV. Kiss *et al.*⁴⁶ report the detection of the giant isoscalar quadrupole resonance in ^{24}Mg at an energy of about 19 MeV, slightly below the expected position of $63/A^{1/3}$ MeV. According to their estimates the observed giant resonance exhausts 40% to 70% of the EWSR. Therefore at most 30% of the EWSR is expected in other regions of excitation.

The agreement between the isoscalar transition rates obtained from the present (p,p') experiment and from the (e,e') measurements for most of the states is very good. This gives one some confidence in using this approach for states which were not resolved in the (e,e') experiments. The transition rates from the (α,α') work of Yang *et al.*³ at 70 MeV have in general higher values than those from the present (p,p') measurements. It has been proposed⁴⁷ that the 8.654 MeV 2^+ state is the first excited state of the rotational band build on the 0^+ state at 6.432 MeV. Thus the contribution of the two-step process may be responsible for the deviation of the angular distribution (Fig. 7) for this rather weakly excited state from the DWBA predictions. Also the shape of the angular distributions for the 10.922 MeV and 11.017 MeV states resemble the $L=4$ transitions rather than those with $L=2$. These states have been observed as resonances in the $^{20}\text{Ne}(\alpha,\gamma)^{24}\text{Mg}$ reaction¹⁸ and have been assigned $J^\pi=2^+$, $T=0$. The E2 branches to the ground state were found to carry strengths of 0.4 and 0.09 s.p.u., respectively. Thus the origin of the discrepancies with the DWBA for these two states is not known at present.

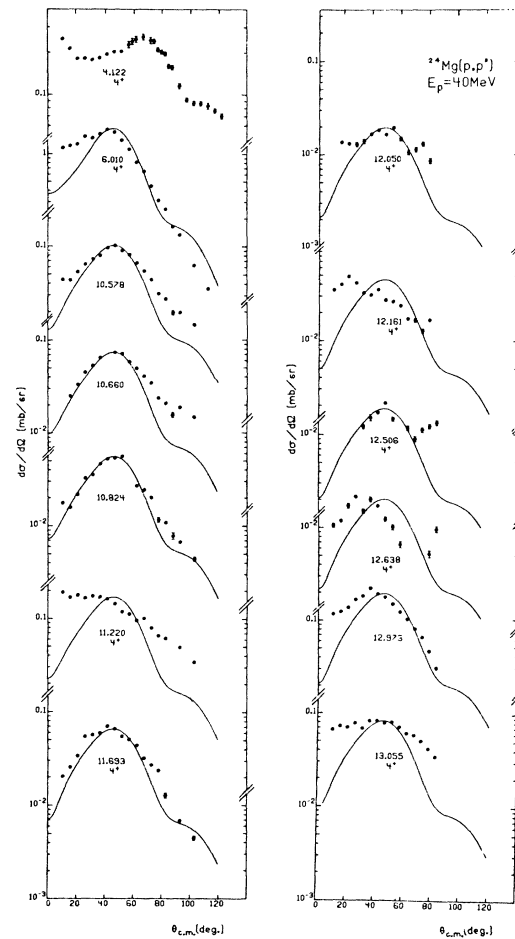


FIG. 10 Angular distributions compared with the DWBA calculations for the angular momentum transfer $L=4$ (solid lines). The normalization coefficients β_L are tabulated in Table II.

Transitions with $L=3$

The transitions to the known and suggested $J^\pi=3^-$ states exhaust 13% of the EWSR limit (see Fig. 13). More than half of the strength is contained in the excitation of the lowest 7.616 and 8.358 MeV states. The ratio of the excitation strengths for these states as found in the present work is $B(8.358 \text{ MeV})/B(7.616 \text{ MeV})=0.78$. A value of 1.6 is found for the same ratio in the (e,e') work by Titze,⁴⁴ 1.5 by Johnston and Drake⁴ and 1.3 is obtained from the (α,α') experiment. The effect does not seem to be dependent on the particular choice of the proton bombarding energy since the 8.358 MeV state was also found to be weaker at $E_p=17.5$ MeV (Ref. 48). However, in both the (e,e') and (α,α') experiments these states are not resolved from nearby 1^- states which probably add to the observed strength. Another possibility is that multi-step processes such as successive pick-up and stripping of a nucleon contribute to the (p,p') excitation of these negative parity states. These would introduce a state dependent interference modifying the intensity ratios from the values seen in (e,e') . Branford *et al.*²⁴ have postulated the existence of two negative parity rotational bands in ^{24}Mg . The 7.616 MeV state is the band-head of the $K^\pi=3^-$ band. The 8.358 MeV state is the first excited

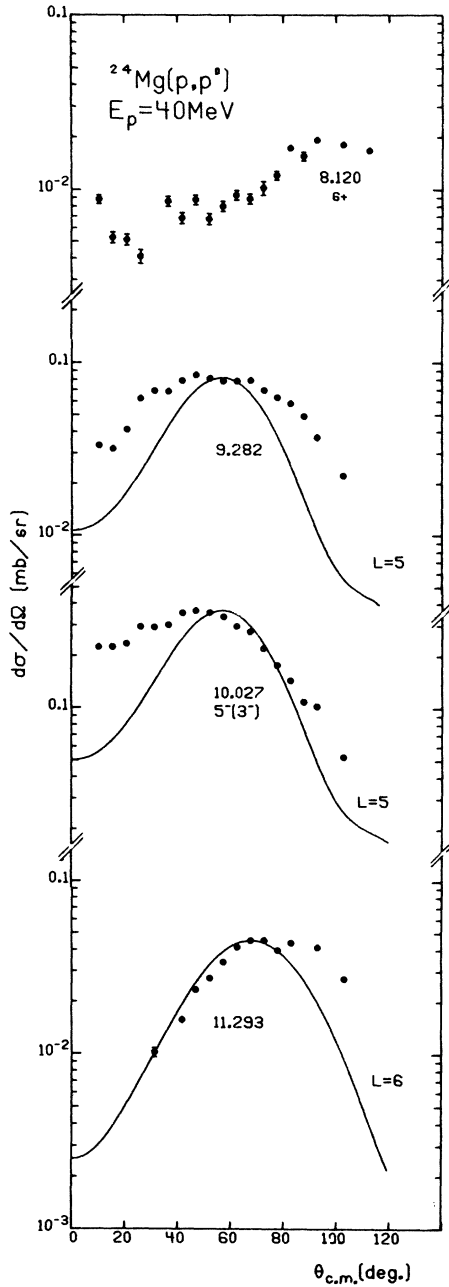


FIG. 11 Angular distributions and the DWBA calculations for the angular momentum transfer $L=5$ and $L=6$. See Sec. V for further details regarding spin-parity assignments.

band member of the $K^\pi=0^-$ band starting at the 7.553 MeV $J^\pi=1^-$ state. The electron data on the higher band members would shed light on the origin of the differences with the (p,p') for the lower states. In the present experiment, the 10.027 MeV $J^\pi=5^-$ ($K^\pi=0^-$) state is strongly excited while the 11.597 MeV $J^\pi=5^-$ ($K^\pi=3^-$) state is barely seen.

The remaining octupole strength observed is distributed among the states grouped around an excitation energy of 12.5 MeV (see Fig. 12).

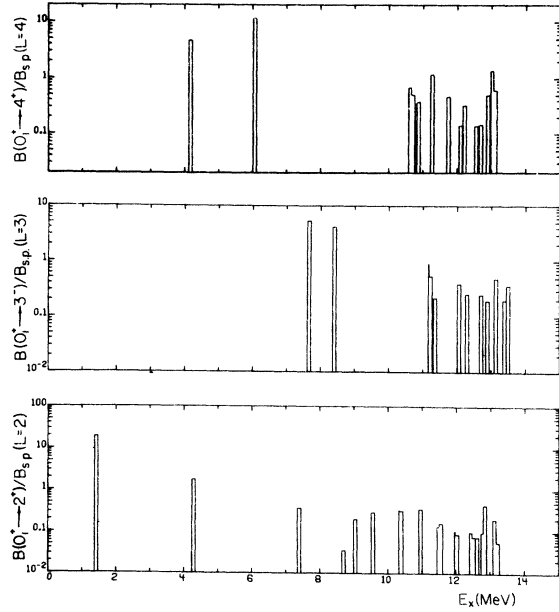


FIG. 12 Distribution of the isoscalar transition strength (expressed in single-particle units $B_{s.p.}(L)$) for the multiplicities $L=2,3$ and 4 as a function of the excitation energy E_x in ^{24}Mg .

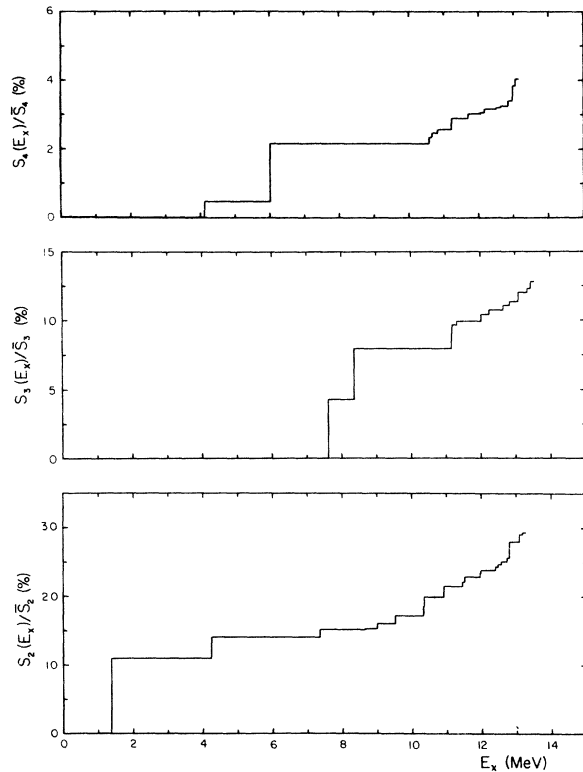


FIG. 13 Fraction of the energy-weighted sum-rule (EWSR) limit S_L/\bar{S}_L (in %) exhausted by the transitions observed up to an excitation energy E_x in ^{24}Mg as a function of E_x for the multiplicities $L=2,3$ and 4 .

Transitions with $L=4$

The percentage of the strength exhausted by the observed transitions below $E_x=13.5$ MeV rapidly decreases with increasing multipolarity. The observed transitions with $L=4$ exhaust only 4.0% of the EWSR limit (see Fig. 13). The strongest transition is the one to the 6.014 MeV state (Fig. 12). This one and the transition to the 4.122 MeV state which is excited primarily by double excitation carry more than half of the observed strength. In contrast to the rather uniform distribution of the strength in the high-energy group for the quadrupole and octupole transitions the states at 11.220 MeV and 12.973 MeV are quite strongly excited compared with the other high lying 4^+ states.

There is a noticeable gap between 6 MeV and 10.5 MeV of excitation where no $L=4$ strength is observed. It is tempting to suggest that for the particle-hole components of the higher 4^+ states the particle transitions occur across two major shells.

Transitions with $L \geq 5$

Only a very small fraction of the EWSR limit (0.3%) is contained in the transition to the $J^\pi=5^-$ state at 10.027 MeV. Partial waves up to about ten only are strongly influenced by the nuclear potential of the magnesium nucleus at this bombarding energy. Therefore the excitation of high-spin states is suppressed. The other known $J^\pi=5^-$ states are at $E_x=11.594$, 13.07 MeV (Ref. 25), 13.86 and 14.14 MeV (Ref. 49). States with spins ranging from 5 to 9 have been excited⁵⁰ in the $^{12}\text{C}(^{16}\text{O},\alpha)$ Mg reaction in the excitation energy range from 12 to 17 MeV. These are not excited with a significant intensity in the present work.

VIII. SUMMARY

The inelastic scattering of protons from ^{24}Mg nucleus has been studied at the proton energy $E_p=40$ MeV with a resolution of the order of 15 keV. The excitation energy range from the ground state up to $E_x=13.6$ MeV has been covered. Excitations of two types, particle-hole and collective have been encountered. The excitations of the former type are found to have a characteristic bell shaped angular distributions.

The angular distributions for the scattering from the natural-parity $T=0$ states have been compared with the

predictions of the macroscopic collective model. The macroscopic collective model was used with the DWBA theory to determine the deformation parameters β_L and the isoscalar transition rates $B(IS; 0_1^+ \rightarrow L)$. These are tabulated in Table II. Overall, the simple DWBA predictions are in reasonable agreement with the experimental angular distributions for many states with $L=2$ and higher multiplicities. The lowest multiplicities ($L=0$ and $L=1$) probably require a microscopic approach in order to extract quantitative information. Satisfactory agreement was obtained with transition rates from electron scattering data at low excitations. This gives some credence to the transition rates found for the higher excitation region ($E_x=8-13.5$ MeV) in which the resolution attainable at present with the electron scattering is insufficient to determine the strength of the individual transitions. For the three multiplicities $L=2$, $L=3$ and $L=4$ this energy region was found to contribute nearly half of the observed strength. The angular distributions for the ground-state $K^\pi=0^+$ rotational band members have been measured up to and including the 6^+ state at 8.120 MeV. The data were compared with the predictions of the coupled-channel calculations assuming the rigid-rotor model for the ground-state rotational band. The comparison corroborates the conclusion that the hexadecapole moment of ^{24}Mg is very small ($|\beta_4|=0.03$). It is not possible to state conclusively whether β_4 is positive or negative. Because of the small size of the hexadecapole deformation, the $J^\pi=6^+$ state is mainly excited by the three-step $L=2$ and one-step $L=6$ angular momentum transfers and thus one can draw some tentative conclusions about the deformation of the sixth order. The data tend to exclude positive values of β_6 since they give destructive interference with the three-step excitation. For a value of $\beta_6=-0.0175$, the magnitude, but not the position, of the backward maximum is reproduced. It would be necessary to refine the model in order to attempt more detailed agreement with the data.

Acknowledgements

One of us (B.Z.) wants to express his sincere gratitude to Professor H. Blosser for the hospitality extended to him during his stay at the Cyclotron Laboratory. Thanks are due Dr. C.H. King for help with the coupled-channel calculations.

* Work supported by the U.S. National Science Foundation.

† On leave from the Institute of Nuclear Research, Warsaw, Poland.

¹J. Eenema, R.K. Cole, C.N. Waddel, H.S. Sandhu and R.R. Dittman, Nucl. Phys. **A218**, 125(1974).

²A. Kiss, O. Aspelund, G. Hrechuss, K.T. Knopfle, M. Rogge, U. Schwinn, Z. Seres, P. Turek and C. Mayer-Boricke, Nucl. Phys. **A262**, 1(1976).

³G.C. Yang, P.P. Singh, A. van der Woude and A.G. Drentje, Phys. Rev. **C13**, 1376(1976).

⁴A. Johnston, and T.E. Drake, J. Phys. A: Math., Nucl., Gen. **7**, 898(1974).

⁵A.V. Cohen and J.A. Cookson, Nucl. Phys. **29**, 604(1962).

⁶H. Rebel, G.W. Schweimer, G. Schatz, J. Specht, R. Lohken, G. Hauser, D. Habs and H. Klewe-Nebenius, Nucl. Phys. **A182**, 145(1972).

⁷P.M. Endt and C. van der Leun, Nucl. Phys. **A214**, 1(1973).

⁸B. Ziegliniski, G.M. Crawley, J.A. Nolen, Jr., and H. Nann, Bull. Am. Phys. Soc. **22**, 28(1977).

⁹R.G. Markham and R.G.H. Robertson, Nucl. Instr.

and Meth. **129**, 131(1975).

¹⁰J.R. Comfort, University of Pittsburgh (unpublished).

¹¹C.E. Moss, Nucl. Phys. **A269**, 429(1976).

¹²G.C. Hamilton and L.N. Vance, Michigan State University, Cyclotron Laboratory (unpublished).

¹³P. Schwandt, University of Wisconsin (1967) (unpublished).

¹⁴F.D. Becchetti and G.W. Greenlees, Phys. Rev. **182**, 1190(1969).

¹⁵P.D. Kunz, University of Colorado (unpublished).

¹⁶S.F. Biagi, W.R. Phillips and A.R. Barnett, Nucl. Phys. **A242**, 160(1975).

¹⁷E. Goldberg, W. Haerberli, A.I. Galonsky and R.A. Douglas, Phys. Rev. **93**, 799(1954).

¹⁸P.J.M. Smulders, Physica **31**, 973(1965).

¹⁹R.H. Spear and I.F. Wright, Aus. J. Phys. **21**, 307(1968).

²⁰G.J. Highland and T.T. Thwaites, Nucl. Phys. **A109**, 163(1968).

²¹H. Fuchs, K. Grabisch, P. Kraaz and G. Roschert, Nucl. Phys. **A122**, 59(1968).

- ²²S.M. Tang, B.D. Sowerby and D.M. Sheppard, Nucl. Phys. A125, 289(1969).
- ²³B. Zwiaglinski, G.M. Crawley, W. Chung, J.A. Nolen, Jr., and H. Nann, to be published.
- ²⁴D. Branford, N. Gardner and I.F. Wright, Phys. Lett. 36B, 456(1971).
- ²⁵J.L.C. Ford, Jr., J. Gomez de Campo, R.D. Robinson, P.H. Stelson and S.T. Thornton, Nucl. Phys. A226, 189(1974).
- ²⁶R.W. Ollerhead, J.A. Kuehner, R.J.A. Levesque and E.W. Blackmore, Can. J. Phys. 46, 1381(1968).
- ²⁷M.A. Meyer, J.P.L. Reinecke and D. Reitmann, Nucl. Phys. A185, 625(1972).
- ²⁸J. Szucs, B.Y. Underwood, T.K. Alexander and N. Anyas-Weiss, Nucl. Phys. A212, 293(1973).
- ²⁹U.E.P. Berg, K. Wienhard and H. Wolf, Phys. Rev. C 1 1851(1975).
- ³⁰A.S. Keverling Buisman--Thesis (1976), University of Groningen (unpublished).
- ³¹C.D. Porterfield and R.C. Ritter, Bull. Am. Phys. Soc. 12, 553(1967).
- ³²G.F. Neal and S.T. Lam, Phys. Lett. 45B, 127(1973).
- ³³G.S. Adams et al., Bull. Am. Phys. Soc. 21, 966(1976). G.S. Adams et al., Phys. Rev. Lett. 38, 1387(1977).
- ³⁴H. Zarek et al., Phys. Rev. Lett. 38, 750(1977).
- ³⁵W.J. Stark, P.M. Cockburn and R.W. Krone, Phys. Rev. C 1, 1752(1970).
- ³⁶P.D. Kunz, University of Colorado (unpublished).
- ³⁷N. Austern and J.S. Blair, Ann. Phys. 33, 15(1965).
- ³⁸A.M. Bernstein, in Advances in Nuclear Physics, edited by H. Baranger and E. Vogt (Plenum, New York 1969), Vol. III, p. 325.
- ³⁹G.R. Satchler, Nucl. Phys. A100, 481(1967).
- ⁴⁰G.R. Satchler, Part. and Nucl. 5, 105(1973).
- ⁴¹H.P. Morsch, D. Dehnhardt and T.K. Li, Phys. Rev. Lett. 34, 1527(1975).
- ⁴²S. Fuji, Progr. Theor. Phys. 42, 416(1969).
- ⁴³D.S. Onley, Nucl. Phys. A149, 197(1970).
- ⁴⁴O. Titze, Z. Phys. 220, 66(1969).
- ⁴⁵A. Nakada and Y. Torizuka, J. Phys. Soc. Japan 32, 1(1972).
- ⁴⁶A. Kiss, C. Mayer-Boricke, N. Rogge, P. Turek and S. Wiktor, Phys. Rev. Lett. 37, 1188(1976).
- ⁴⁷F. Leccia, H.M. Leonard, D. Castera, P. Hubert and P. Mennrath, J. de Phys. 34, 147(1973).
- ⁴⁸G.M. Crawley and G.T. Garvey, Phys. Rev. 160, 981(1967).
- ⁴⁹L.R. Greenwood, K. Katori, R.E. Malmin, T.H. Braid, J.C. Stoltzfus and R.H. Siemssen, Phys. Rev. C 6, 2112(1972).
- ⁵⁰A. Gobbi et al., Phys. Rev. Lett. 26, 396(1971).